Proceedings of the 7th Manufacturing Engineering Society International Conference – Vigo (Spain) – June 2017

Surface roughness assessment after different strategy patterns of ultrasonic ball burnishing

R. Jerez-Mesa[(1)], G. Gomez-Gras[(2)], J.A. Travieso-Rodriguez[(1)]

[(1)] Departament d'Enginyeria Mecànica. Universitat Politècnica de Catalunya. Escola d'Enginyeria de Barcelona Est. Av. d'Eduard Maristany, 10-14. 08019 Barcelona. e-mail: ramon.jerez@upc.edu
[(2)] Universitat Ramon Llull. IQS School of Engineering. Via Augusta 390, 08017 Barcelona.

ABSTRACT

Ball burnishing is a comprehensive finishing process consisting on deforming plastically a certain surface by the action of a rolling sphere-shaped indenter. In this work, an AISI 1038 workpiece is burnished in two phases. The first phase covers the burnishing of a 10x10 mm patch, performed along the direction of the previous milling. The second pass is applied on the previous patch, following three different strategies, namely, parallel, perpendicular and at a 45-degrees angle with regards to that first burnishing direction. The comparison between the non-vibration assisted ball burnishing (NVABB) and vibration-assisted ball burnishing (VABB) effects is included in the study. To assess the influence of these strategies on the final roughness profile, an L9 Taguchi orthogonal array is designed, including as factors the vibrations amplitude, the burnishing force, and the lateral pass width. Surface roughness is measured and compared to determine the optimal burnishing orientation. The VABB process proves to be more effective in surface roughness improvement. Technical recommendations are given to select the best process parameters inside the tested levels for each factor. All burnishing strategy prove to have different effects on the surface, and should be selected according to the preferential burnishing direction and in service application of the part.

Keywords: ball burnishing, ultrasonic vibrations, steel, surface roughness, Taguchi

1. Introduction

Ball burnishing is a comprehensive finishing process consisting on deforming plastically a certain surface by the action of a rolling sphere-shaped indenter. The complexity of the process is due to a dual fact. Firstly, the high difficulty of modeling plastic deformation phenomena itself. Secondly, the high number of parameters implied in the process, such as burnishing force, number of passes, lateral pass width, etc.

This paper explores two aspects that have been scarcely tackled with in the bibliography. The first one is the vibration-assisted ball burnishing (VABB) process. This process takes advantage of the acoustoplasticity effect, that is, the decrease in the yield strength of a certain material due to an alternating nature of the deforming force [1]. The VABB system using 2-kHz vibrations has been in depth studied by Travieso-Rodriguez et al. (2015) on steel [2] and aluminum [3] specimens. The tool used for these experiments transmitted an alternating force to the workpiece surface by means of a coil excited by an external device, which would cause the alternative deflection of two plates attached to the burnishing ball [4]. The process showed a substantial increase in surface roughness improvement, as well as a slight improvement in surface hardening due to the ball percussion. Some authors have reported the use of VABB process with ultrasonic vibrations, evaluating results in terms residual stress and surface roughness [5]. However, no comprehensive study about the process has yet been made.

The second unexplored aspect is the influence of the burnishing strategy as a means of improving the final surface roughness of burnished parts. Yet, some transversal related aspects have been partially tackled. Lopez de la Calle et al. (2015) compared the results of continuous burnishing and patch burnishing, concluding that patch burnishing allows a higher productivity (maximizes the feed rate to be applied), but derives in higher surface roughness [6]. Gómez-Gras et al. (2016) defined the optimal lateral pass width between burnishing passes to be applied on steel and aluminum materials in order to optimize the burnishing time with no detrimental effect on surface roughness [7]. This factor is highly important to consider, as materials indented by a sphere tend to flow to the borders of the performed path due to plastic deformation, and these material accumulations must be treated by the adjacent pass so that they do not neutralize the positive effect of burnishing.

At sight of the described circumstance, this paper aims to study the influence of different patterns after a first uniform burnishing phase. For this reason, three different strategies are considered: parallel, perpendicular and at a 45-degrees angle with regards to the first burnishing direction. To make a more comprehensive study, the lateral pass width is added as a second influential factor on the results, as it has proved to be influential as well with regards to surface roughness. In the third place, the burnishing tool used to performed the VABB allows to change the amplitude of the vibration, as a percentage of the maximum amplitude. The non-vibration-assisted process is compared with two VABB processed, each one with different amplitudes. This will allow to know the improvement introduced by vibrations, and whether the amplitude has influence on final results or not. Finally, these three factors are combined with a fourth one, which is the burnishing force, with an already proved influence on roughness results [8].

2. Materials and methods

2.1 Specimens preparation

An AISI 1038 specimen was fixed on a LAGUN 600 CNC milling machined used to perform the experiments. It was surfaced with a 4-teeth milling cutter, using a cutting velocity of 90 m/min, and 400-mm/min feed rate. This previous milling operation allowed to homogenize the departing condition before burnishing, and to guarantee a totally horizontal position of the working surface in order to not to introduce unwanted secondary forces due to uncontrolled change in the spring compression length.

Table I shows the initial surface conditions (average surface roughness R_a and total roughness R_t) of the workpiece, measured along the *x* and *y* direction, by applying a cut-off length λ_c of 0.25 mm, and an evaluation length of 4 mm. The *y* direction refers to the feed direction in the milling operation (Figure 1), which is also the preferential burnishing direction for the first burnishing phase. It is also the burnishing direction for the all first burnishing phases. The *x* direction corresponds to the axis at right angles with the initial burnishing direction, and is to be taken as preferential burnishing direction in the perpendicular strategy for the second burnishing phase.

Table I. *Initial roughness measured at the workpiece surface.*

Direction	R_a (µm)	R_t (µm)
x	1.831	10.463
y	2.107	11.601

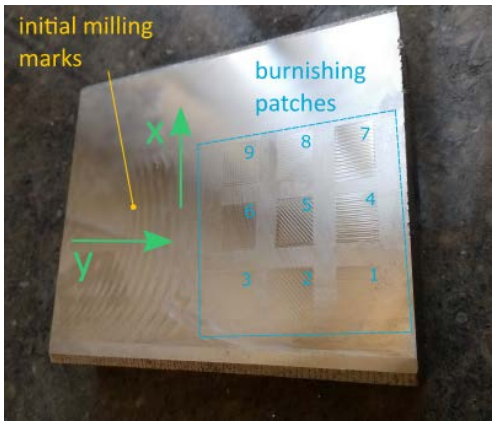

Figure 1. *Burnished workpiece and reference directions referred to in this article.*

2.2 Taguchi experimental design

Four burnishing parameters are to be tested on the prepared specimen, namely, the burnishing force, the burnishing strategy, the lateral pass width, and different amplitudes of the VABB process, coupled with the non-vibration assisted scenario (Table I). These four factors were used to design the experimental phase through an L9 Taguchi array. A partial experimental design was selected due to its adequacy to tackle with preliminary studies as this one.

Table I. *Factors and levels of the Taguchi design*

Factor	Level 1	Level 2	Level 3
Vibrations amplitude	0%	50%	100%
Burnishing strategy	parallel (PAR)	45 degrees (45DEG)	perpendicular (PERP)
Burnishing force (N)	90	180	270
Lateral pass width (mm)	0.35	0.42	0.49

The levels assigned to each factor have been decided as follows:

- **Vibrations amplitude**. This factor considers the shift from the NVABB process to the VABB. The former is modelled through amplitude zero assisting the process, whereas the latter corresponds to 50% and 100% amplitude levels. These values are defined as percentages because of the regulating system defined in the equipment, which is performed through a manual rotary switch.
- **Burnishing strategy**. All nine essays will be executed through a first burnishing phase along the *y* direction, that is, parallel to the milling direction. From that point, a second phase will be performed following three different patterns, coded as PAR, 45DEG and PERP in the DOE matrix. These three levels describe an increasing inclination of the burnishing passes, covering from 0 degrees –parallel strategy– to 90 degrees –perpendicular–, that is, along the *x* direction.
- **Burnishing force.** It was selected according to previous works, where 90 N was a force level causing a desirable plastic deformation of the surface [2]. Two multiples of this level were taken as higher levels, to test the behavior of the material when higher forces are applied. In effect, critical force values are often found in burnishing systems, which prove to be detrimental in terms of roughness improvement.
- **Lateral pass width**. Previous studies also showed optimal lateral pass width to guarantee roughness improvement [7]. Therefore, the lower level for the level lateral pass width factor was set at b_0 = 0.35 mm. The idea of increasing this length as more burnishing passes are performed wants to be explored, and the other two tested levels have been calculated as $1.2b_0$ and $1.4b_0$.

The L9 Taguchi array is a 3^4 array, that is, allows to include a maximum of four parameters at 3 levels, as is done in the experimental setup for this article (Table II). The experiment is therefore saturated, and no column is left for the calculation of error terms. However, as the influence of amplitude, strategy and lateral pass width wants to be assessed in general terms, this experimental design is taken as valid. Future works will allow working with wider experimental arrays to calculate linear models.

Table II. *Taguchi design of experiments*

Exp.	A	strategy	F (N)	b (mm)
1	0	PAR	90	0.35
2	0	45DEG	180	0.42
3	0	PERP	270	0.49
4	50%	PAR	180	0.49
5	50%	45DEG	270	0.35
6	50%	PERP	90	0.42
7	100%	PAR	270	0.42
8	100%	45DEG	90	0.49
9	100%	PERP	180	0.35

The workpiece shall be burnished therefore nine times. Each test comprises a first burnishing phase, in which a 10x10 mm burnishing patch will be performed along the *y* direction. Once the whole burnishing process is performed, R_a and R_t along both the *x* and *y* directions shall be measured with a Mitutoyo Surftest S-210 contact profilometer, and taken as response variables. The surface roughness decrease requires the application of a cutoff length of λ_c of 0.25 mm, and an evaluation length of 1.25 mm, being the diamond head displaced at 5 mm/min along that length.

2.3 Burnishing tool

The utilization and command over the burnishing tool allows to perform the essays following the indications at the experimental plan. The tool head, where the 10-mm diameter burnishing ball is housed, is attached to a piezoelectric module which can be excited through an external generator with a 40-kHz electrical signal. That signal excites the piezoelectric, which vibrates at the same ultrasonic frequency. The burnishing ball, attached to that module, vibrates consequently while rolling on the treated surface during the experiment. A spring inside the tool shaft allows to regulate the burnishing force. The tool can be calibrated through a force cell attached to a universal testing machine, which compresses the tool at a known velocity. That way, time can be turned into length, and a calibration curve is generated from the registered points, as shows Figure 2. This graph gives, for a certain desired burnishing force, the negative

z coordinate to be programmed in the ISO code during the burnishing test. For reasons of confidentiality and industrial transfer, no further detailed information can be provided about the tool construction.

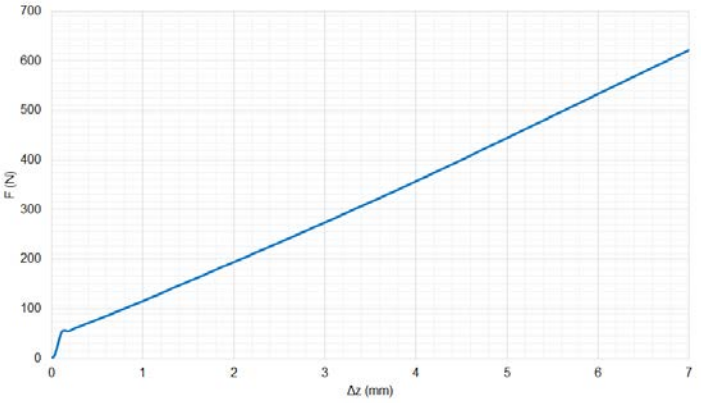

Figure 2. *Calibration curve of the burnishing tool. It fits to a linear equation according to Hooke's Law.*

3. Results discussion

3.1 Surface roughness results

All burnishing tests were performed on the milled surface of the AISI 1038 workpiece. Table III shows the surface roughness descriptors, obtained as average values from samples of ten measurements for each burnishing condition. All samples have been generated by discarding outliers according to the Chauvenet's criterion. Therefore, the average results shown in table III are representative of the whole sample. Through this condition, each value of the samples values does not present relative errors higher than 5% with the regards to their average representative.

Table III. *Surface roughness results measured at the 9 tested burnishing patches.*

Exp.	A	strategy	F (N)	b (mm)	$R_{a,x}$ (µm)	$R_{t,x}$ (µm)	$R_{a,y}$ (µm)	$R_{t,y}$ (µm)	ρ_a	ρ_t
1	0	PAR	90	0,35	0.234	1.069	0.127	0.696	1.842	1.536
2	0	45DEG	180	0,42	0.127	0.800	0.114	0.589	1.114	1.358
3	0	PERP	270	0,49	0.058	0.340	0.200	0.928	0.290	0.366
4	50%	PAR	180	0,49	0.171	0.782	0.044	0.312	3.886	2.506
5	50%	45DEG	270	0,35	0.138	0.582	0.140	0.579	0.986	1.005
6	50%	PERP	90	0,42	0.070	0.486	0.160	0.887	0.438	0.548
7	100%	PAR	270	0,42	0.159	0.742	0.041	0.358	3.975	2.073
8	100%	45DEG	90	0,49	0.121	0.617	0.138	0.627	0.877	0.984
9	100%	PERP	180	0,35	0.052	0.337	0.169	0.689	0.308	0.489

In addition to average and total surface roughness, the *x*-to-*y* roughness ratio, ρ, is calculated and presented at Table III. This ratio describes the relative magnitude of surface roughness valued measured along the *x* direction with respect to the *y* direction eq. (1). Therefore, ρ values near 1 indicate that roughness values measured along *x* and *y* are similar; values much lower than 1 indicate that roughness measured along *y* is much higher than the ones measured along *x*. Last of all, values higher than 1 show the contrary.

$$\rho_i = \frac{R_{i,x}}{R_{i,y}}; i = \{a, t\} \quad (1)$$

These results have been represented at Figure 3, where blue tones show average surface roughness results, and orange bars show total roughness. A first visual inspection leads to conclude that all tested burnishing conditions improve surface roughness with regards to the initial roughness values. Furthermore, the VABB roughness are lower than the ones obtained with the NVABB process. Therefore, the assistance of the burnishing process with ultrasonic vibrations is beneficial in terms of surface roughness improvement.

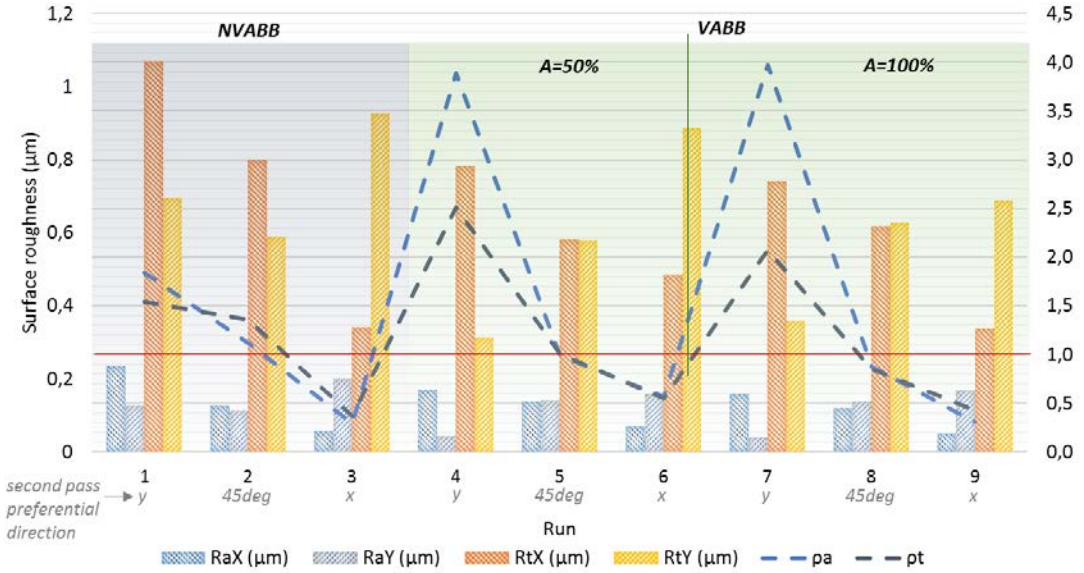

Figure 3. *Surface roughness results for all tested conditions. Blue tones show the average roughness results. Orange tones show total roughness. Red line represents ρ = 1.*

Secondly, the *x*-to-*y* ratio evolution for both average roughness and total roughness shows that the relative relation between these parameters measured along both directions follows the same pattern. On the other hand, only in the essays #3, #6 and #9, $\rho < 1$. That means that surface roughness is relatively more improved along the *y* axis in the essays were the second pass is along the *x* axis. The complementary can be explained for $\rho > 1$, corresponding to essays #1, #4 and #7. The tested conditions for these burnishing imprints include the second pass along the *y* axis, which was the direction of all passes. $\rho \approx 1$ at essays where the strategy pattern was at 45 degrees. At sight of these results, it seems that the final burnishing pass dominates the preferential direction for roughness improvement; and, that it is the same direction as that final pass. The direction of the previous milling and the first pass are not influential in the final results in terms of relative improvement.

3.2 ANOVA analysis

Statistical processing of the results is necessary to evaluate the actual significance of what has been so far observed. On the other hand, a more comprehensive study allows to represent the influence of each factor on the response, and the robustness associated to that influence. An analysis of variance (ANOVA) test has been, running the DOE and its results on the Minitab 17 software. The main effects plot has been represented for every measured surface roughness as response variable. The S/N ratio has been calculated considering the smaller is better scenario, as the objective is to minimize the resulting surface roughness (eq. 2).

$$\frac{S}{N} = -10 \cdot \log\left(\sum \frac{Y^2}{n}\right) \tag{2}$$

Figure 4 shows the effects plot for $R_{a,x}$. The strategy proves to be the most influential factor on this result, which agrees with what was already observed and explained at section 3.1. The VABB process shows a lower surface roughness, bigger as the amplitude of the vibration increases. As for the force, 180 N seems to achieve the lowest surface roughness, and at the sight of the results, increasing the force to 270 N does not show special improvement. Much on the contrary, it can lead to undesired higher friction forces. Last of all, the lateral pass width of 0.49 mm shows the best results, although the difference with regards to 0.42 mm is not substantial. At sight of the S/N ratios effects plot, the highest values correspond to the factor levels where the response is minimized, which is the objective. The optimal tested levels are, therefore, the most robust ones for the $R_{a,x}$.

Results for $R_{a,y}$ are shown at Figure 5. Conclusions are similar as the ones explained for $R_{a,x}$, although this variable proves to be more influenced by the force, so that a 270 N force is not advisable, as it is detrimental for the average roughness result. The lateral pass width also shows a threshold value which

should not be exceeded if average roughness should not be harmed. The VABB process also shows a roughness improvement with regards to NVABB.

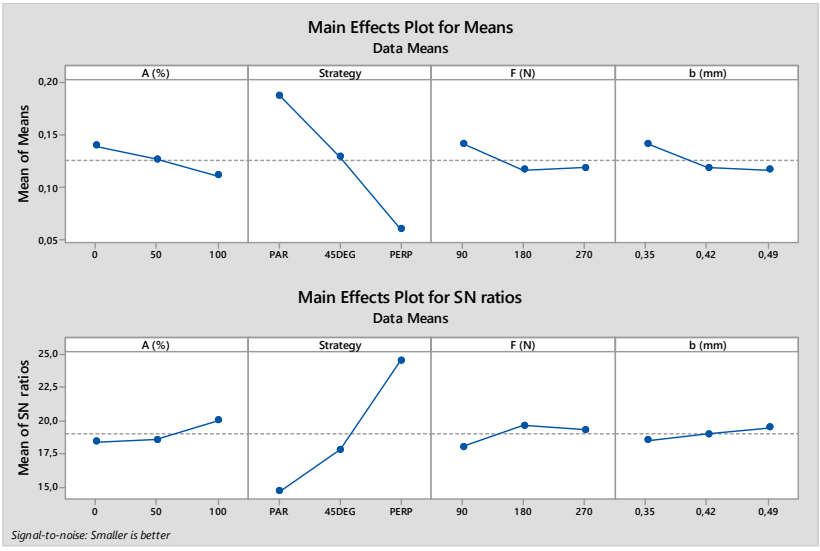

Figure 4. *Effect plots for means and S/N ratios. Response variable:* $R_{a,x}$.

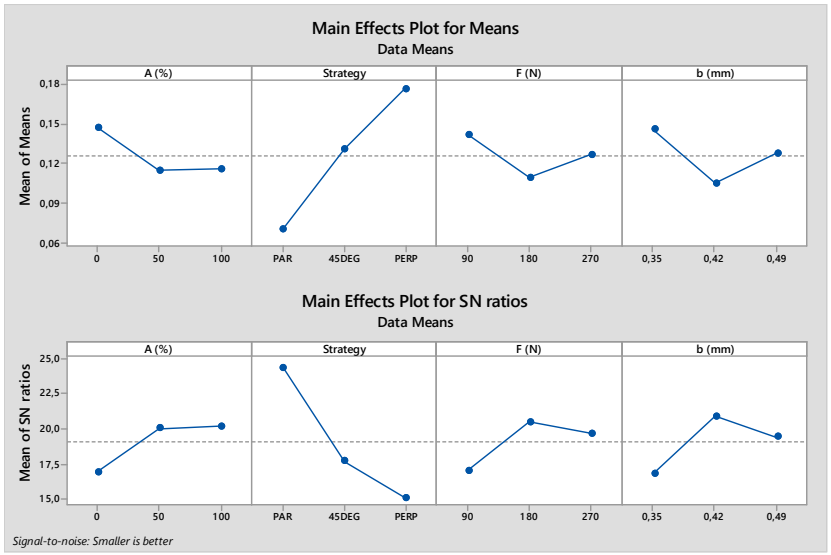

Figure 5. *Effect plots for means and S/N ratios. Response variable:* $R_{a,y}$.

The results of total roughness are represented at figures 6 and 7. A similar pattern can be found for both variables. First of all, the strategy is the most influential parameter. As was already observed, the lowest total roughness is observed when measured along the direction of the second and last pass. The VABB process also proves to diminish total roughness, although increasing the amplitude from 50% does not show a significant effect on the response. Agreeing to what has been concluded for average roughness, total roughness also shows a threshold value for the burnishing force and lateral pass width, which are detrimental to total roughness. A 270-N force and 0.49-mm lateral pass width show the highest total roughness than their immediately lower levels. It makes sense if we imagine that a higher force can provoke more material flow to the boundaries of the burnishing imprint, and, as the following burnishing pass is performed at nearly 0.5 mm of the first one, that material is not deformed by the adjacent pass, and generates a new peak in the surface, higher than the previous one. This effect is not detected in terms

of average surface roughness. Robustness also agrees positively with mean effect in these total roughness results.

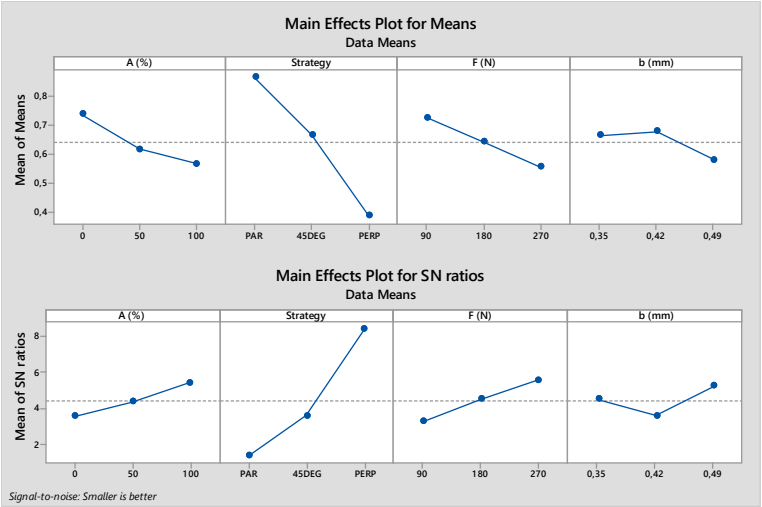

Figure 6. *Effect plots for means and S/N ratios. Response variable: $R_{t,x}$.*

Figure 7. *Effect plots for means and S/N ratios. Response variable: $R_{t,y}$.*

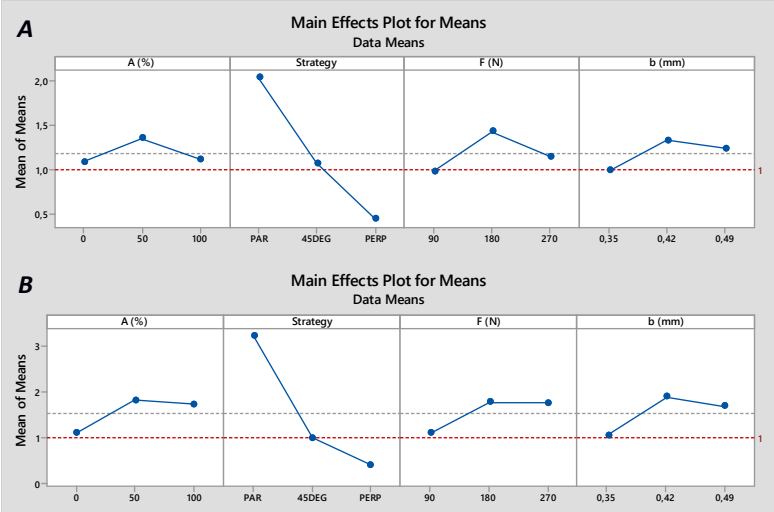

Figure 8. *Effect plots for means and S/N ratios. Response variable: (A) ρ_a. (B) ρ_t .*

4. Conclusions

An AISI 1038 specimen has been burnished through the NVABB and VABB processes, by applying different strategies, forces and lateral pass width between adjacent passes. Average and total surface roughness have been measured along the initial milling direction and the perpendicular one. The following conclusions can be drawn:

1. The direction of the last burnishing pass dominates the magnitude of the surface roughness results on the workpiece, resulting the lowest values along the direction of that last pass. The strategy should therefore be decided according to the in-service work regime of the burnished part.
2. The VABB of AISI 1038 proves to derive in lower surface roughness values with respect to the NVABB. Furthermore, as the amplitude value increases, the overall effect is more conspicuous.
3. Critical values of force and lateral pass width have been found, from which total roughness can be worsened. This effect is not present when considering average surface roughness. Table IV shows the best burnishing values found from the discussed experimental design.

Table IV. *Technical recommendation for VABB process to improve average and total roughness on AISI 1038.*

A	F	b (mm)	strategy			
100%	180 N	0.42 mm	**Objective:**	Improve initial milling direction (*y*)	Improve direction at 90 degrees of initial milling direction (*x*)	Balanced roughness improvement in both directions
			Then use strategy:	PAR	PERP	45DEG

5. Acknowledgements

This study is financially supported by the Ministry of Economy and Competitiveness of Spain through grant DPI2015-69803-R, and is greatly appreciated.

6. References

[1] K.W. Siu, A.H. Ngan, I.P. Jones. New insight on acoustoplasticity–Ultrasonic irradiation enhances subgrain formation during deformation. International Journal of Plasticity, 27, 5, 788-800, 2011.

[2] J.A. Travieso-Rodriguez, G. Gomez-Gras, G. Dessein, F. Carrillo, J. Alexis, J. Jorba-Peiro, N. Aubazac. Effects of a ball-burnishing process assisted by vibrations in G10380 steel specimens. The International Journal of Advanced Manufacturing Technology, 81, 9-12, 1757-1765, 2015.

[3] J.A. Travieso-Rodríguez, G. Gomez-Gras, J. Jorba-Peiró, F. Carrillo, G. Dessein, J. Alexis,H. Gonzalez-Rojas. Experimental study on the mechanical effects of the vibration-assisted ball-burnishing process. Materials and Manufacturing Processes, 30, 12, 1490-1497, 2015.

[4] G. Gómez-Gras, J.A. Travieso-Rodríguez, H.A. González-Rojas, A. Nápoles-Alberro, F. Carrillo, G. Dessein (2015). Study of a ball-burnishing vibration-assisted process. Proceedings of the Institution of Mechanical Engineers, Part B: Journal of Engineering Manufacture, 229, 1, 172-177, 2015.

[5] A.T. Bozdana, N.N.Z. Gindy. Comparative experimental study on effects of conventional and ultrasonic deep cold rolling processes on Ti–6Al–4V. Materials Science and Technology, 24, 11, 1378-1384, 2008.

[6] L.N. López de Lacalle, A. Rodriguez, A. Lamikiz, A. Celaya, R. Alberdi. Five-axis machining and burnishing of complex parts for the improvement of surface roughness. Materials and Manufacturing Processes, 26, 8, 997-1003 ,2011.

[7] G. Gomez-Gras, J.A. Travieso-Rodriguez, R. Jerez-Mesa, J. Lluma-Fuentes, B. Gomis de la Calle. Experimental study of lateral pass width in conventional and vibrations-assisted ball burnishing. The International Journal of Advanced Manufacturing Technology, 87, 1-4, 363-371, 2017.

[8] J.A. Travieso-Rodríguez, G. Dessein, H.A. González-Rojas. Improving the surface finish of concave and convex surfaces using a ball burnishing process. Materials and Manufacturing Processes, 26, 12, 1494-1502, 2011.